An Improved SEIR Model Considering the Impact of Contact-Restricting Policies: A Case Study of COVID-19 in Wuhan

Silu Chen
Wuhan University
Jiangping Chen (chen_jp@whu.edu.cn)
Wuhan University
Tianyou Cheng
Wuhan University

Research Article

Keywords: Q-SEIR, COVID-19, Epidemic model, Contact-restricting, Dynamic contact rate, Numerical simulation

Posted Date: August 4th, 2021

DOI: https://doi.org/10.21203/rs.3.rs-715229/v1

Abstract

Dynamic modeling of infectious disease can simulate transmission processes of COVID-19, a newly been found infectious respiratory disease that has a substantial impact on both people's health and social development, and therefore plays an important role in the prediction and prevention of epidemics. Although there are many models that can accurately represent the number of infected patients, the influence of human factors on the transmission of the virus has not been fully investigated. Here, by considering the influence of policies on restricting contact between people, we modified the SEIR infectious disease model and developed a new model called the Quarantine-considering SEIR model (hereafter referred to as Q-SEIR), combining with dynamic parameter, contact rate, obtained by machine learning method, we can represent the effects of human movement and contact behavior during the epidemic.

The experimental results show that this method can effectively represent the effect of patterns of population activity on the development of the epidemic. On one hand, our research results provide guidance for the government before issuing measures to restrict the movement and socialization of people; and on the other hand, our findings help identify the development stage of the epidemic more clearly for the public as well as provide information for citizens' travel decisions.

1 Introduction

Since December 2019, an outbreak in Wuhan caused by COVID-19 has greatly affected both the health of citizens and the development of society [1,2]. Compared with other familiar respiratory infectious diseases, COVID-19 has a higher rate of infection, and in the early stages, can manifest as mild symptoms. These characteristics make COVID-19 more difficult to detect and thus more likely to infect additional individuals [3,4]. To contain the outbreak as soon as possible, the government not only has to make efforts in medical treatment, but also accurately predict the potential losses. Under such difficult circumstances, Wuhan, as the first city that reported cases, has taken many new measures to curb the spread of the virus, such as movement restrictions. According to the Oxford COVID-19 Government Response Tracker (OxCGRT) released by Oxford University[5], these movement-restricting measures range from stipulations on wearing masks, to the establishment of Fangcang hospitals that isolate infectious people, to a national lockdown [6]. These measures can efficiently cut off the route of transmission of the virus by limiting people's interpersonal contact. Studies have shown that the lockdown of Wuhan, combined with emergency response measures, prevented more than 700,000 infections throughout China [7]. However, these measures will produce some side effects. For example, a series of problems, including social instability, are likely to occur if such policies restricting people's freedom of travel are strictly implemented.

Therefore, it is necessary to have a tool that can accurately simulate and predict the progress of the virus in a certain area under the influence of local policies, in order to provide guidance for both the government and the public. An analysis of COVID-19 in Wuhan is a suitable case study for researching

the virus and estimating the effectiveness of movement-restricting policies due to the quality of the available data and the presence of strictly implemented measures [8]. This research can not only be used as a reference for other countries and regions, but also help governments react more quickly when facing other diseases in the future.

Modeling epidemics is fundamental to having an understanding of the progress of the disease and evaluating the efficacy of new strategies for its containment [9–11]. Thus far, many classical models have been used to simulate epidemics [12–16]. The autoregressive integrated moving average (ARIMA) model was used by Domenico Benvenuto et al. [17]. In some circumstances, this method can generate accurate results, but it is reliant on timely past data, which is not available at the start of an epidemic. The SEIR model divides people into four compartments: susceptible, exposed, infectious, and removed [18]; it has been applied to many virus outbreaks such as MERS [19,20] and SARS [21,22], which established its public prominence [23–25]. However, as these classical models do not consider the unique features of COVID-19, many studies have built upon them by introducing new parameters or new groups into the existing models to represent more types of population, which can assist in representing reality more accurately [26–28].

Considering that COVID-19, as a respiratory infectious disease, its transmission depends on the contact between people. This contact can be influenced by many human factors, including the wearing of masks and city lockdown. Therefore, some studies have modelled the effect of quarantine in limiting contact between people by introducing the contact rate into classical models to improve the simulation results. For example, Kiesha Prem et al. constructed synthetic contact matrices for different age groups based on the classic SEIR model to reflect the impact of city lockdown on contact rates [29]. Nevertheless, it is not ideal to set a constant contact rate because its value is likely to fluctuate with the development of the epidemic [30–33]. To allow for this, Jia Wangping et al. added a transmission modifier π (t) to represent a time-varying contact rate [34].

It is important to note that variation of the parameters is often achieved by setting different values manually at different time periods (similar to piecewise functions), yet this approach still has certain limitations. First, the number of time periods is limited. Second, there are some parameters, such as contact rate, for which there are no official statistics. Thus, using a machine learning method to calculate the dynamic parameters is an appealing method. By introducing the key parameter as a function of time into the SIRD model, Duccio Fanelli et al. could more accurately reflect the effect of city lockdown on the spread of the epidemic [35]. Thus far, some studies have adopted a least squares method to fit the value of the parameters [36–38]; however, the gradient descent method has the advantage of being able to represent a non-linear relationship between parameters. With that in mind, even though the gradient descent algorithm requires more computation, it remains an appropriate method to obtain the parameters.

This study proposes a new infectious disease dynamics model that fully considers the transmission features of COVID-19 and the influence of government policies on the progress of the epidemic. This work

also applies a more flexible machine learning method to obtain key parameters that can be used to model the progress of the epidemic.

2 Methods

2.2 Q-SEIR model based on relevant policy in Wuhan

COVID-19 is notable for having some special transmission features [3,4,39]. And there are some policies adopted by the Wuhan government and some human factors that may affect the epidemic, including 14 days of quarantine for suspected infected persons. Therefore, our assumptions for the Q-SEIR model combine the transmission features of COVID-19 and role of policies that restrict the movement and contact between people on the prevention and control of the epidemic

Due to these conditions, we subdivided the compartments of the traditional SEIR model according to whether an individual can freely move around and be in contact with other people. To do this, S (susceptible) was divided into S (susceptible) and Q_S (quarantined susceptible); E (exposed) was divided into E (exposed) and Q_E (quarantined exposed); and I (infected) was divided into I (infected) and H (hospitalized). In the SEIR model, recovered and dead patients are all referred to as R (removed). Lastly, we divided the removed population into R (recovered) and D (dead) groups.

The definition of each compartment is given below:

S(t): number of individuals susceptible to being infected at time t.

E(t): number of exposed individuals who are asymptomatic or have not manifested symptoms at time t; this group is able to infect others.

I(t): number of infected individuals who are not hospitalized and can infect others at time t.

R(t): number of individuals who have recovered at time t.

QS(t): number of susceptible individuals who are under quarantine and thus cannot come into contact with other people at time t.

QE(t): number of exposed individuals who are under quarantine so that they will not come into contact with other people at time t.

H(t): number of individuals who are being treated in hospital at time t.

D(t): cumulative number of individuals who have died due to the disease, up to time t.

The interactions among the different stages of infection are shown in Fig. 1.

The evolution of the population in each stage can be described in a set of differential equations:

$$\dot{S}(t) = \gamma_3 \cdot Q_S(t) - \beta_1 \cdot S(t) - c(t) \cdot \frac{\mu_1 \cdot E(t) + \mu_2 \cdot I(t)}{E(t) + I(t)} \cdot S(t)$$

$$\dot{Q}_S(t) = \beta_1 \cdot S(t) - \gamma_3 \cdot Q_S(t)$$

$$\dot{E}(t) = c(t) \cdot \frac{\mu_1 \cdot E(t) + \mu_2 \cdot I(t)}{E(t) + I(t)} \cdot S(t) - (\beta_2 + \alpha) \cdot E(t)$$

$$\dot{Q}_E(t) = \theta \cdot R(t) + \beta_2 \cdot E(t) - \alpha \cdot Q_E(t)$$

$$\dot{I}(t) = \alpha \cdot E(t) - (\sigma + d_1) \cdot I(t)$$

$$\dot{H}(t) = \sigma \cdot I(t) + \alpha \cdot Q_E(t) - (\gamma_2 + d_2) \cdot H(t)$$

$$\dot{R}(t) = \gamma_2 \cdot H(t) - \theta \cdot R(t)$$

$$\dot{D}(t) = d_1 \cdot I(t) + d_2 \cdot H(t)$$

Here, the uppercase Latin letters represent the change in the populations during a unit interval of time (considering the simulation duration and simulation accuracy of the Q-SEIR model, here, we set 1 day as the unit interval).

The parameters are defined as follows:

μ1, μ2: the probability of a susceptible individual being infected due to contact with an infectious person (where μ1 denotes contact with an exposed person and μ2 denotes contact with an infected person, respectively). In previous studies, μ1 was usually smaller than μ2 [40].

α: probability of a susceptible or quarantined susceptible person showing symptoms per unit time.

β1, β2: transmission rate of an individual under quarantine due to local policy. β1 and β2 denote the rate of transition from S to Q_S, and from E to Q_E, respectively.

γ1, γ2: recovery rates for an infected individual and a hospitalized individual, respectively. The recovery rate is assumed to vary during the course of the epidemic.

γ3: rate of individuals being released from quarantine. This parameter is in consideration of the local policy, when the quarantined individuals are deemed not to be infected after a certain period of screening, they will be released and are free to move about.

d1, d2: mortality rates of self-treating infected individuals and hospitalized individuals, respectively. This parameter, like the recovery rate, can also change over time.

σ: due to limited medical resources, only some of the infected people can be treated in hospital at any one time. This parameter presents the probability that an infected individual can be treated in hospital.

θ: due to the possibility of inaccurate test results, some partially recovered patients may still test positive. This parameter represents the transmission rate of recovered individuals in comparison with quarantined

exposed individuals.

c(t): the contact rate, that is, the number of individuals that a given person comes into contact with per unit time. The transmission routes of COVID-19 mainly include direct transmission, aerosol transmission, and contact transmission. All these routes of transmission require close human contact. In this paper, we deem that when such contact occurs between one person and another, it becomes a valid contact between those two individuals.

2.3 Parameter estimation in the Q-SEIR model

We divide the parameters into two categories, simple parameters and complex parameters. The values of simple parameters are set manually while the values of complex parameters are calculated by an algorithm. Table 1 shows the assignment of all the simple parameters. In addition, by February 15, the proportion of severe cases within the confirmed cases in Wuhan had decreased significantly, so we chose February 15 as the critical time point. By considering the availability of data on the parameters as well as their dynamic variability, we set different values for σ and γ2 before and after February 15, so as to achieve a more accurate simulation.

Table 1

Numerical values and physical interpretation of the simple parameters involved in Q-SEIR

Parameters	Numerical Value
γ1	0.0098
γ2	0.0098 (Jan 25th to Feb 15th), 0.1 (after Feb 15th)
γ3	0.0714
σ	0.1 (Jan 25th to Feb 15th), 0.2 (after Feb 15th)
Θ	0.0002
A	0.156
d1	0.001
d2	0.0019
β1	0.00005
β2	0.015
μ1	0.063
μ2	0.041

As the key parameter in this model, the effective contact rate is calculated using an algorithm to obtain the function of its variation with time. Gradient descent is a popular and simple method in machine learning, and there are two variations on the classical gradient descent method: SGD (stochastic gradient descent) and BGD (batch gradient descent). In BGD, all the sample points are applied at once to calculate the gradient. Although this method is simpler than SGD, it has the limitation that when the dataset is large, the speed of descent can be slow and the optimal solution may not always be obtained. Conversely, SGD only uses one randomly selected sample point to calculate the derivative each time. As a result, SGC can achieve faster convergence. It is worth mentioning that normally, standard SGD is uniformly differentiated and applied across all parameters. However, in this study, there were significant differences in the amount of data available for different variables. For example, the data on the number of hospital inpatients covers only about 20 days, which is far less than the statistics on the number of confirmed patients. In this case, it can lead to problems such as unbalanced influence between different parameters. Hence AdaGrad was applied to deal with these problems. The AdaGrad optimizer adapts the learning rate of model parameters independently by scaling each parameter inversely to the square root of the sum of all its past gradient averages. The parameters with the maximum gradient of the cost function have a correspondingly rapid decrease in learning rate, while the parameters with a small gradient have a relatively small decrease in learning rate. Therefore, AdaGrad applies a small learning rate for the more prevalent category of data and a large learning rate when the data is limited; thus, AdaGrad is suitable for datasets with a sparse or unbalanced data distribution, which means it is more suitable for the calculation of contact rate in this study.

Second, the initial value of each group must be set. At the beginning of the epidemic, the medical system in Wuhan was not fully prepared and it did not record all the necessary data and statistics. In consequence, the data from the early stages of the epidemic are not fully sufficient for our study. Therefore, in order to ensure that the model simulation covers the entire period of interest, we simulated data from January 23 to February 11 and from February 12 to April 10 separately, causing the parameters to be set twice. The assignment is shown in Table 2.

Table 2

Numerical values and physical interpretation of the initial number of each population compartment involved in our Q-SEIR model

Group	Initial Value (Start on Jan 25th)	Initial Value (Start on Feb 12th)
R	40	1,915
I	533	16,031
H	0	14,004
E	0	23,194
QE	0	2,207
QS	0	2,697
S	6,211,382	6,150,916
D	45	1,036

3 Results

3.1 Contact rate of COVID-19 in Wuhan

The curves for the contact rate in Wuhan are shown in Fig. 2. Panel (a) shows the contact rate with infectious individuals (curve c_Inf), while panel (b) shows the contact rate with any individual (curve c_All). Both curves suddenly increase on February 12, which may be caused by limited data availability in the early stages followed by an abrupt change in the number of confirmed cases on this day.

The curve for the contact rate from January 25 to February 11 had little fluctuation due to the relatively short duration. Starting from February 12, c_Inf began to decline until it was close to zero. By comparison, the variation for c_All is more complex. This may be because infected patients were being treated, so the probability of identifying new cases was decreasing. Meanwhile, as the movement of people was restricted by measures such as quarantine and city lockdown, c_All also decreased accordingly. Due to the strict management measures and good cooperation from the population, c_All began to decline. Finally, after the epidemic was suppressed, c_All slowly began to increase again; however, it was still significantly lower than its level on February 1 (approximately 1.6).

By cross referencing with news reports, March 13 was the first day on which there were no new suspected cases in Hubei province [41], and starting from March 14, public passenger transport, together with some businesses in low-risk areas began to operate. April 8 is the date when the lockdown of Wuhan was fully lifted [42]. It is apparent that several time points in the calculated contact rate curve, where the trends of contact rate changes, correspond to real events, indicating that our simulation results are in line with reality and are accurate.

3.2 Simulation results of different population compartments in Wuhan

Figure 3 shows the simulation results over two time periods. It is worth mentioning that there is a sudden increase in each population on February 12 due to the revision in the diagnosis [43]. Moreover, there is no obvious discrepancy in the number of recoveries and deaths, which is consistent with reality, indicating that the accuracy of our model is relatively high. However, different populations have different patterns of change under the impact of the increasing level of I. In addition, the range of change of compartments S, E, and H are larger than those of R, QS, QE, and D. We postulate that the larger numbers of these groups may lead to more pronounced fluctuations in their numbers.

Overall, compartments I and H began to show a downward trend at the end of February and maintained a low level from the beginning of April. Conversely, E and QE began to decline after February 12, by which time most of the active cases had been reported. The emergence of this short time lag between these groups may be accredited to the government's ongoing discovery of latent patients and of patients in self-isolation. There is a relatively longer time lag between I and R due to the time needed to treat patients.

We also selected RMSE and R^2 as indexes to evaluate the accuracy of the simulation. Taking the simulation of Wuhan from February 12 to April 10, 2020 as an example, the RMSE was 496.096 and the R^2 was 0.99873. We also simulated the results without the AdaGrad optimizer, as shown in Fig. 4. The results obtained using the AdaGrad algorithm are better than those without AdaGrad.

To verify that the proposed model can be used in other locations, we applied the Q-SEIR model to simulate data from Italy over the period March 10 to June 15. The results are shown in Fig. 5. The overall variation within each population is very similar to the results from Wuhan. By June, the numbers in compartments I and H in Italy began to decline, while those for R and H continued to increase. This indicates that if Italy can maintain the current epidemic prevention measures without the influence of other external causes, there is a good possibility that the epidemic in Italy can be contained.

3.3 Estimation of the impact of restricting contact between people

To verify that lowering the population contact rate has a significant impact on epidemic prevention and control, we simulated a situation where, other things being equal, the date of the city lockdown was delayed (shown in Fig. 6). We assumed that when no movement restriction measures were implemented, contact among people (i.e., the contact rate) remained unchanged at the simulated level on January 25. After the measures were taken, the contact rate changed according to the original simulation results (shown in Fig. 2). Results indicate that when the implementation date is delayed, the time to reach the peak of the epidemic is delayed, and the number of confirmed cases at the peak is much higher than the original values. In addition, the change in the number of patients does not vary linearly with the postponement of the lockdown date. The increasing trend of the number of patients will be faster with each postponement of the closure date. We find that without the movement restriction policies, the

outbreak would have lasted for more than 50 days when assuming other factors were unchanged. Under these conditions, its peak would have resulted in 3.5 million people falling ill.

In further experiments, we also simulated the outbreak in Italy to evaluate the best date for its city lockdown. We simulated the scenarios of advances of 3 days, 5 days, 7 days, 9 days, and 11 days (the results are shown in Figure S1). Although the maximum number of infectious people will decrease with the advance of the date of lockdown, the rate of decline in the number of infectious people will be slower as the number of days advance. Hence, it would be optimal to bring the date of lockdown forward by about 3 days.

4 Discussion

In this paper, we proposed the Q-SEIR model to represent the time-dependent transmission pattern of COVID-19. The groups in this model are derived from the compartments of the traditional SEIR model with new compartments to represent the mobility of people, so that the model is extended to include susceptible, exposed, infected, recovered, susceptible under quarantine, exposed under quarantine, hospitalized, and dead. One of the key parameters, the contact rate, was obtained by applying a machine-learning-based method, and other dynamic parameters were manually selected at various time periods. The experimental results show that the model can obtain accurate simulation results and can be easily extended to other areas. The research results not only reflect the regularities of patterns of movement and contact between people during an epidemic through the calculation of the contact rate, but also reveal and allow for the existence of many cases that were not counted during the epidemic. The proposed method can thus be used as a tool to respond to the development stage of the epidemic and provide guidance for travel restrictions, as well as to effectively guide the government to implement relevant policies such as city lockdown and quarantine schedules.

The key feature of our Q-SEIR model is the distinction between those who are allowed to move around and those who are restricted, which can be further subdivided into quarantined and unquarantined healthy individuals, quarantined and unquarantined latent individuals, and quarantined and unquarantined patients (i.e., self-treating and hospitalized patients). Such a distinction, on one hand, can enable the community to quantify the prevalence of disease within complex data, such as different types of people with different transmission rates and mortality rates. On the other hand, this distinction can also enable us to focus on different populations of people with different mobility characteristics, such as individuals in quarantine isolated from the rest of the population, while others are free to move around and come into contact with other people. Therefore, the proposed model can explain and quantify the direct impact of the city lockdown on population movement restrictions as well as the differences in the development of the epidemic.

5 Conclusion

The spread of COVID-19 in a certain region can be expected to show some regularity. It is of great significance for the control and prevention of COVID-19 to explore its development and mode of transmission, especially to identify the key features that affect its spread. To better understand this, our approach modifies the classical SEIR model and proposes a new dynamic infectious disease model, known as Q-SEIR; its contributions are as follows.

1) The unique features of COVID-19, measures implemented by governments, and limited medical resources were considered to develop this improved model. Although the initial experiments were focused on Wuhan, we also showed that the proposed Q-SEIR model could be extended to other regions such as Italy.

2) In this study, using the gradient descent algorithm and AdaGrad optimizer to calculate the dynamic contact rate was found to be effective. By introducing a dynamic contact rate and subdividing the population compartments of the SEIR model according to mobility, we can consider the influence of population movement and interpersonal contact on the progress of infectious diseases. According to the experimental results, we found that government interventions will affect the movement and contact rates within the population, which will subsequently affect the spread of infectious diseases.

3) The Q-SEIR model can effectively guide the formulation of epidemic prevention strategies. When an infectious virus spreads in a certain region, the Q-SEIR model can enable the government to simulate the possible development of the epidemic in advance and to consider whether movement restrictions are necessary.

4) Through the simulations of contact rate for different population compartments, the public can gain a better understanding of the current stage of the epidemic, thereby allowing them to make better informed travel decisions.

6 Data Availability

Various types of data were used in this study such as epidemic topics, demographics, and news reports. Taking Wuhan as an example, Table 3 lists the sources of data we used to determine the parameters and initial values in our Q-SEIR model.

Table 3

Sources of data corresponding to the situation in Wuhan (from January 25th to April 10th, 2020)

Descriptions of the Data	Source
Epidemiological data of Wuhan	The notification of the outbreak released by the official website of the Wuhan Health Commission (http://wjw.wuhan.gov.cn/ztzl_28/fk/yqtb/) [43]
Total population of Wuhan	Wuhan Resident Population Statistics in 2019 (https://s.askci.com/news/hongguan/20200330/0905011158591.shtml) [44]
Number of people who left Wuhan on the day of the lockdown	Interview with the mayor of Wuhan on January 26, 2020 (https://www.thepaper.cn/newsDetail_forward_5644624) [45]
Number of confirmed cases among suspected cases	Interview with the mayor of Wuhan on January 26, 2020 (https://www.thepaper.cn/newsDetail_forward_5644624) [46]
Probability of infection after contact between infected and exposed populations	Epidemiological characteristics of infection in COVID-19 close contacts in Ningbo city [40]
The incubation period of COVID-19	Incubation period of 2019 novel coronavirus (2019-nCoV) infections among travelers from Wuhan, China, 20–28 January 2020 [47]
Hospitalization data in Wuhan from February 5 to February 25, 2020	Official website of the Wuhan Health Commission (http://wjw.wuhan.gov.cn/front/web/list3rd/yes/803) [48]
Data related to the positive occurrence of Nucleic Acid	Tencent news (https://new.qq.com/omn/20200708/20200708A0T6IW00.html) [49] and related papers [50,51]

7 Declarations

Acknowledgements

The authors are grateful to the Wuhan Health Commission and the Protezione Civile for supplying the data for this study.

Author contributions

C.S. designed the study, collected essential data, and wrote the manuscript. C.T. was in charge of preprocessing the data and performing the model simulation. C.J. supervised the experiments and revised the manuscript. All authors discussed and interpreted the results and reviewed the manuscript.

Competing interests

The authors declare no competing interests.

8 References

1 Fernandes, N. Economic effects of coronavirus outbreak (COVID-19) on the world economy. *Available at SSRN 3557504* (2020).

2 Chakraborty, I. & Maity, P. COVID-19 outbreak: Migration, effects on society, global environment and prevention. *Science of the Total Environment*, 138882 (2020).

3 Zeidler, A. & Karpinski, T. M. SARS-CoV, MERS-CoV, SARS-CoV-2 comparison of three emerging Coronaviruses. *Jundishapur Journal of Microbiology***13** (2020).

4 Zhu, Z. *et al.* From SARS and MERS to COVID-19: a brief summary and comparison of severe acute respiratory infections caused by three highly pathogenic human coronaviruses. *Respiratory research***21**, 1-14 (2020).

5 *COVID-19 GOVERNMENT RESPONSE TRACKER*, <https://www.bsg.ox.ac.uk/research/research-projects/covid-19-government-response-tracker> (

6 Burki, T. China's successful control of COVID-19. *The Lancet Infectious Diseases***20**, 1240-1241 (2020).

7 Tian, H. *et al.* The impact of transmission control measures during the first 50 days of the COVID-19 epidemic in China. *MedRxiv* (2020).

8 *Hubei: Ensure the data is open and transparent, and the confirmed cases are not allowed to be censored*, <https://new.qq.com/omn/20200221/20200221A0QAUX00.html> (

9 He, S., Peng, Y. & Sun, K. SEIR modeling of the COVID-19 and its dynamics. *Nonlinear Dynamics***101**, 1667-1680 (2020).

10 Hou, C. *et al.* The effectiveness of quarantine of Wuhan city against the Corona Virus Disease 2019 (COVID-19): A well-mixed SEIR model analysis. *Journal of medical virology* (2020).

11 Li, Q., Tang, B., Bragazzi, N. L., Xiao, Y. & Wu, J. Modeling the impact of mass influenza vaccination and public health interventions on COVID-19 epidemics with limited detection capability. *Mathematical Biosciences*, 108378 (2020).

12 Ribeiro, M. H. D. M., da Silva, R. G., Mariani, V. C. & dos Santos Coelho, L. Short-term forecasting COVID-19 cumulative confirmed cases: Perspectives for Brazil. *Chaos, Solitons & Fractals*, 109853 (2020).

13 Cooper, I., Mondal, A. & Antonopoulos, C. G. A SIR model assumption for the spread of COVID-19 in different communities. *Chaos, Solitons & Fractals***139**, 110057 (2020).

14 Barlow, N. S. & Weinstein, S. J. Accurate closed-form solution of the SIR epidemic model. *Physica D: Nonlinear Phenomena*, 132540 (2020).

15 Alzahrani, S. I., Aljamaan, I. A. & Al-Fakih, E. A. Forecasting the spread of the COVID-19 pandemic in Saudi Arabia using ARIMA prediction model under current public health interventions. *Journal of infection and public health***13**, 914-919 (2020).

16 Papastefanopoulos, V., Linardatos, P. & Kotsiantis, S. COVID-19: A Comparison of Time Series Methods to Forecast Percentage of Active Cases per Population. *Applied Sciences***10**, 3880 (2020).

17 Benvenuto, D., Giovanetti, M., Vassallo, L., Angeletti, S. & Ciccozzi, M. Application of the ARIMA model on the COVID-2019 epidemic dataset. *Data in brief*, 105340 (2020).

18 *Compartmental models in epidemiology*, <https://en.wikipedia.org/wiki/Compartmental_models_in_epidemiology> (

19 Kwon, C.-M. & Jung, J. U. Applying discrete SEIR model to characterizing MERS spread in Korea. *International Journal of Modeling, Simulation, and Scientific Computing***7**, 1643003 (2016).

20 Chowell, G., Blumberg, S., Simonsen, L., Miller, M. A. & Viboud, C. Synthesizing data and models for the spread of MERS-CoV, 2013: key role of index cases and hospital transmission. *Epidemics***9**, 40-51 (2014).

21 Godio, A., Pace, F. & Vergnano, A. SEIR Modeling of the Italian Epidemic of SARS-CoV-2 Using Computational Swarm Intelligence. *International Journal of Environmental Research and Public Health***17**, 3535 (2020).

22 Teles, P. A time-dependent SEIR model to analyse the evolution of the SARS-CoV-2 epidemic outbreak in Portugal. *arXiv preprint arXiv:2004.04735* (2020).

23 Cao, J., Jiang, X. & Zhao, B. Mathematical modeling and epidemic prediction of COVID-19 and its significance to epidemic prevention and control measures. *Journal of Biomedical Research & Innovation***1**, 1-19 (2020).

24 Yang, Z. *et al.* Modified SEIR and AI prediction of the epidemics trend of COVID-19 in China under public health interventions. *Journal of Thoracic Disease***12**, 165 (2020).

25 Wang, L. *et al.* Modelling and assessing the effects of medical resources on transmission of novel coronavirus (COVID-19) in Wuhan, China. *Mathematical Biosciences and Engineering***17**, 2936-2949 (2020).

26 Roda, W. C., Varughese, M. B., Han, D. & Li, M. Y. Why is it difficult to accurately predict the COVID-19 epidemic? *Infectious Disease Modelling* (2020).

27 Peng, T., Liu, X., Ni, H., Cui, Z. & Du, L. City Lockdown and Nationwide Intensive Community Screening Are Effective In Controlling COVID-19 Epidemic: Analysis Based on A Modified SIR Model. (2020).

28 Giordano, G. *et al.* Modelling the COVID-19 epidemic and implementation of population-wide interventions in Italy. *Nature Medicine*, 1-6 (2020).

29 Prem, K. *et al.* The effect of control strategies to reduce social mixing on outcomes of the COVID-19 epidemic in Wuhan, China: a modelling study. *The Lancet Public Health* (2020).

30 *Timeline | 76 days of wuhan "city closure" events*, <https://www.thepaper.cn/newsDetail_forward_6869742> (

31 Wuhan metro bus taxis resumed operation on April 22.

32 Tantrakarnapa, K., Bhopdhornangkul, B. & Nakhaapakorn, K. Influencing factors of COVID-19 spreading: a case study of Thailand. *Journal of Public Health*, 1-7 (2020).

33 e Silva, R. d. F. & Pitzurra, R. What are the factors influencing the COVID-19 outbreak in Latin America? *Travel Medicine and Infectious Disease* (2020).

34 Wangping, J. *et al.* Extended SIR prediction of the epidemics trend of COVID-19 in Italy and compared with Hunan, China. *Frontiers in medicine***7**, 169 (2020).

35 Fanelli, D. & Piazza, F. Analysis and forecast of COVID-19 spreading in China, Italy and France. *Chaos, Solitons & Fractals***134**, 109761 (2020).

36 Sarkar, K., Khajanchi, S. & Nieto, J. J. Modeling and forecasting the COVID-19 pandemic in India. *Chaos, Solitons & Fractals***139**, 110049 (2020).

37 Sahoo, B. K. & Sapra, B. K. A data driven epidemic model to analyse the lockdown effect and predict the course of COVID-19 progress in India. *Chaos, Solitons & Fractals***139**, 110034 (2020).

38 Wickramaarachchi, W. & Perera, S. An SIER model to estimate optimal transmission rate and initial parameters of COVD-19 dynamic in Sri Lanka. *Alexandria Engineering Journal* (2020).

39 Dao, T. L. & Gautret, P. Recurrence of SARS-CoV-2 viral RNA in recovered COVID-19 patients: a narrative review. *European Journal of Clinical Microbiology & Infectious Diseases*, 1-13 (2020).

40 Yi, C. *et al.* The epidemiological characteristics of infection in close contacts of COVID-19 in Ningbo city. (2020).

41 *Zero new suspected cases were reported in Wuhan on Thursday, experts said, adding that zero should not relax its vigilance*, <https://baijiahao.baidu.com/s?id=1661120557435027485&wfr=spider&for=pc> (

42 2020 Schedule for wuhan city, Hubei Province.

43 *Notification of the outbreak*, <http://wjw.wuhan.gov.cn/ztzl_28/fk/yqtb/> (

44 *Wuhan Statistics Bulletin in 2019: The total GDP was 1622.3 billion, and the resident population increased by 131,000*, <https://s.askci.com/news/hongguan/20200330/0905011158591.shtml> (

45 *Mayor of Wuhan: Five million people have left China due to the Spring Festival and the epidemic*, <https://www.thepaper.cn/newsDetail_forward_5644624> (

46 *Wuhan mayor: The number of confirmed cases could rise by another 1,000 or so*, <http://www.bjnews.com.cn/news/2020/01/26/679968.html> (

47 Backer, J. A., Klinkenberg, D. & Wallinga, J. Incubation period of 2019 novel coronavirus (2019-nCoV) infections among travellers from Wuhan, China, 20–28 January 2020. *Eurosurveillance* **25**, 2000062 (2020).

48 <http://wjw.wuhan.gov.cn/front/web/list3rd/yes/803> (

49 *Follow-up of 651 COVID-19 patients in Wuhan after discharge: no transmission was found in 3% of patients undergoing reexposure*, <https://new.qq.com/omn/20200708/20200708A0T6IW00.html> (

50 Bongiovanni, M. *et al.* The dilemma of COVID-19 recurrence after clinical recovery. *The Journal of Infection* (2020).

51 Gousseff, M. *et al.* Clinical recurrences of COVID-19 symptoms after recovery: viral relapse, reinfection or inflammatory rebound? *Journal of Infection* **81**, 816-846 (2020).

Figures

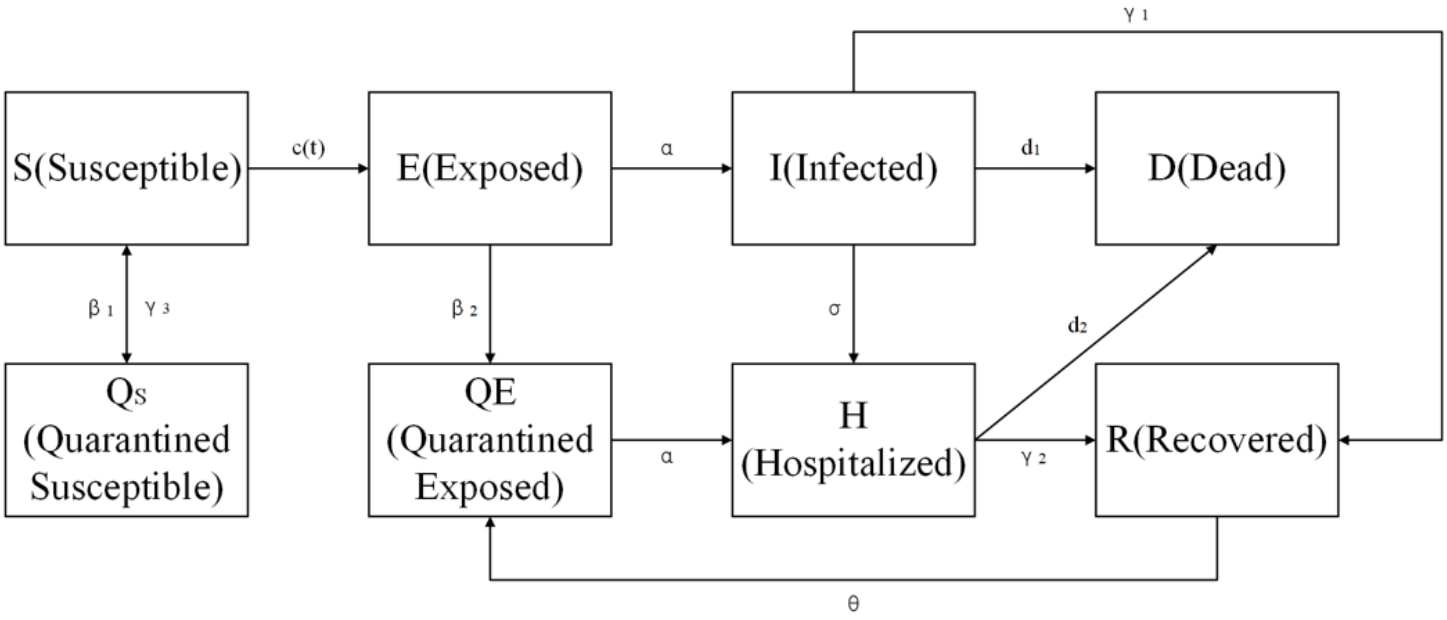

Figure 1

Diagram of the Q-SEIR model

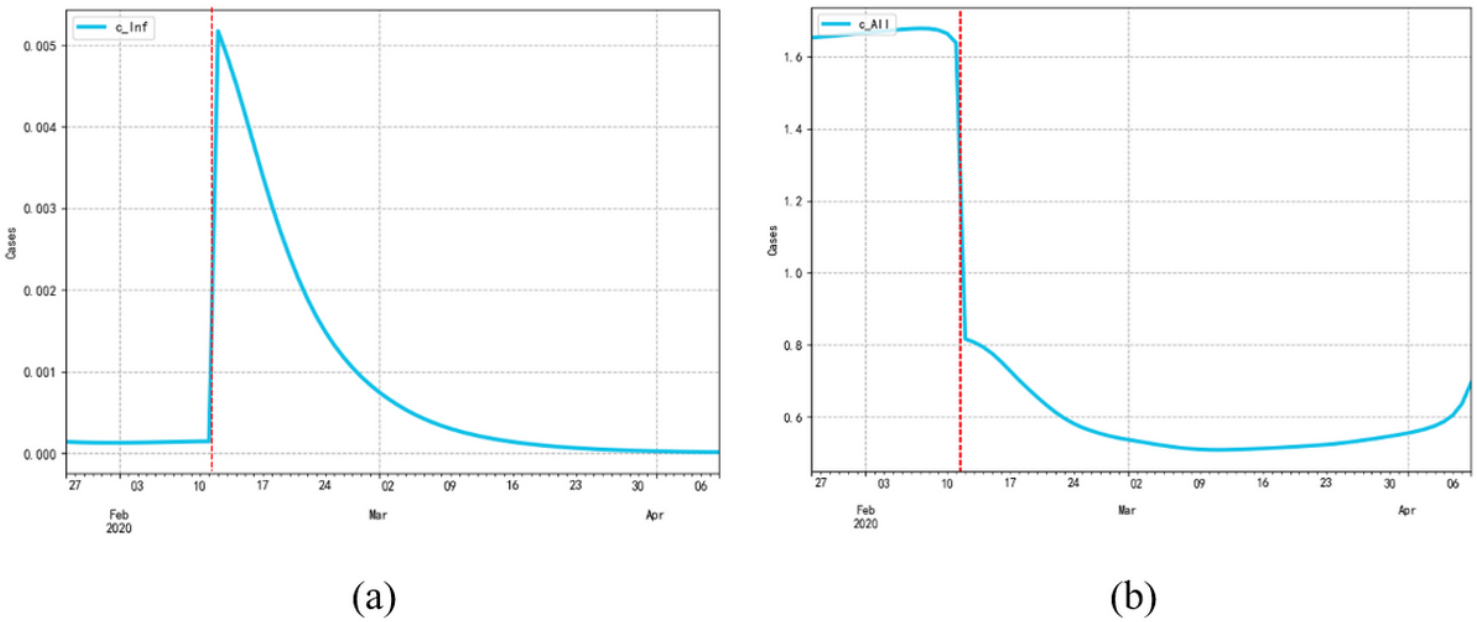

Figure 2

Contact rate in Wuhan. Panel (a): the number of infectious individuals that an individual may come into contact with on a given day. Panel (b): the number of individuals that an individual may come into contact with on a given day.

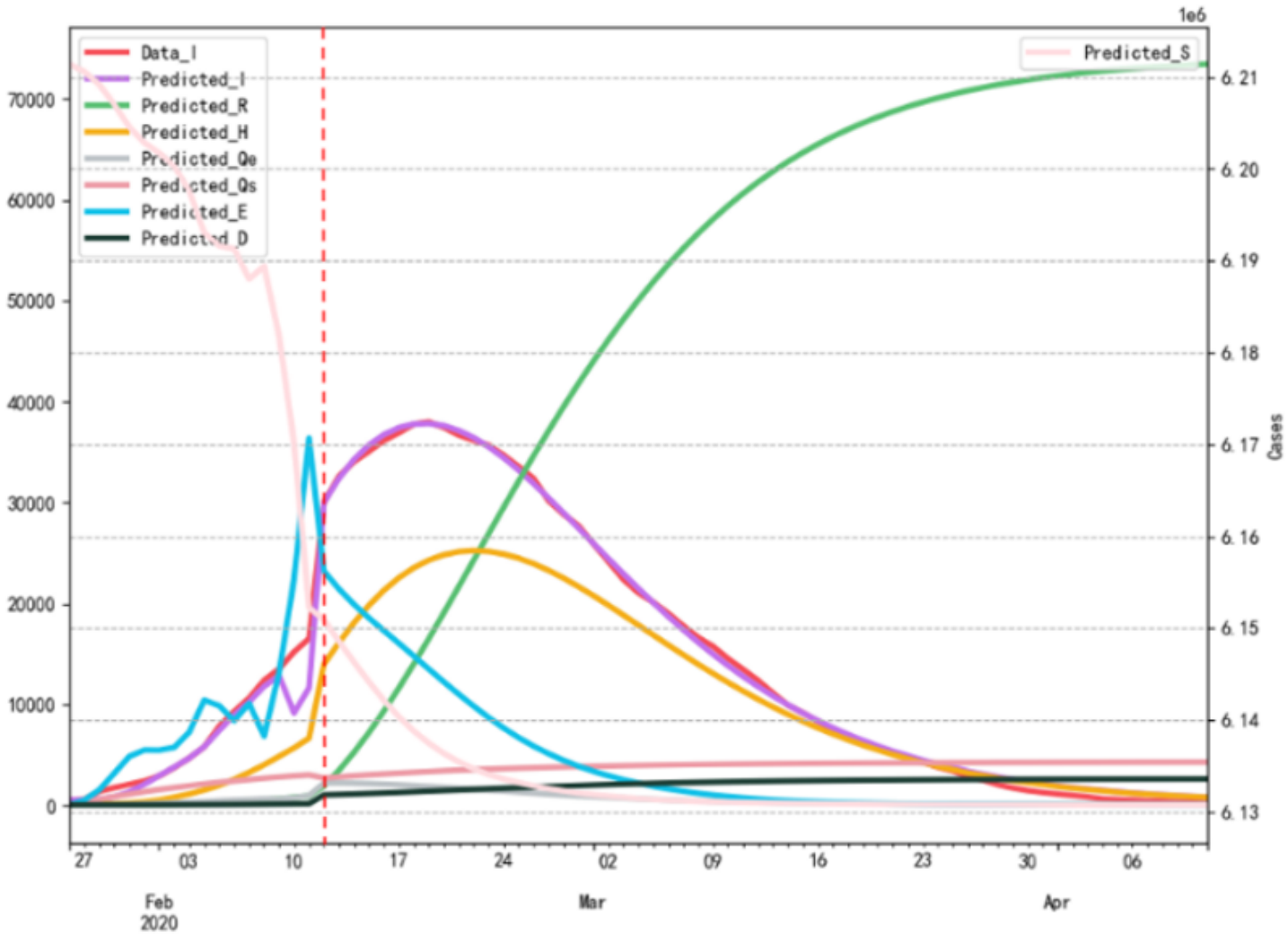

Figure 3

Simulation results for various groups in Wuhan

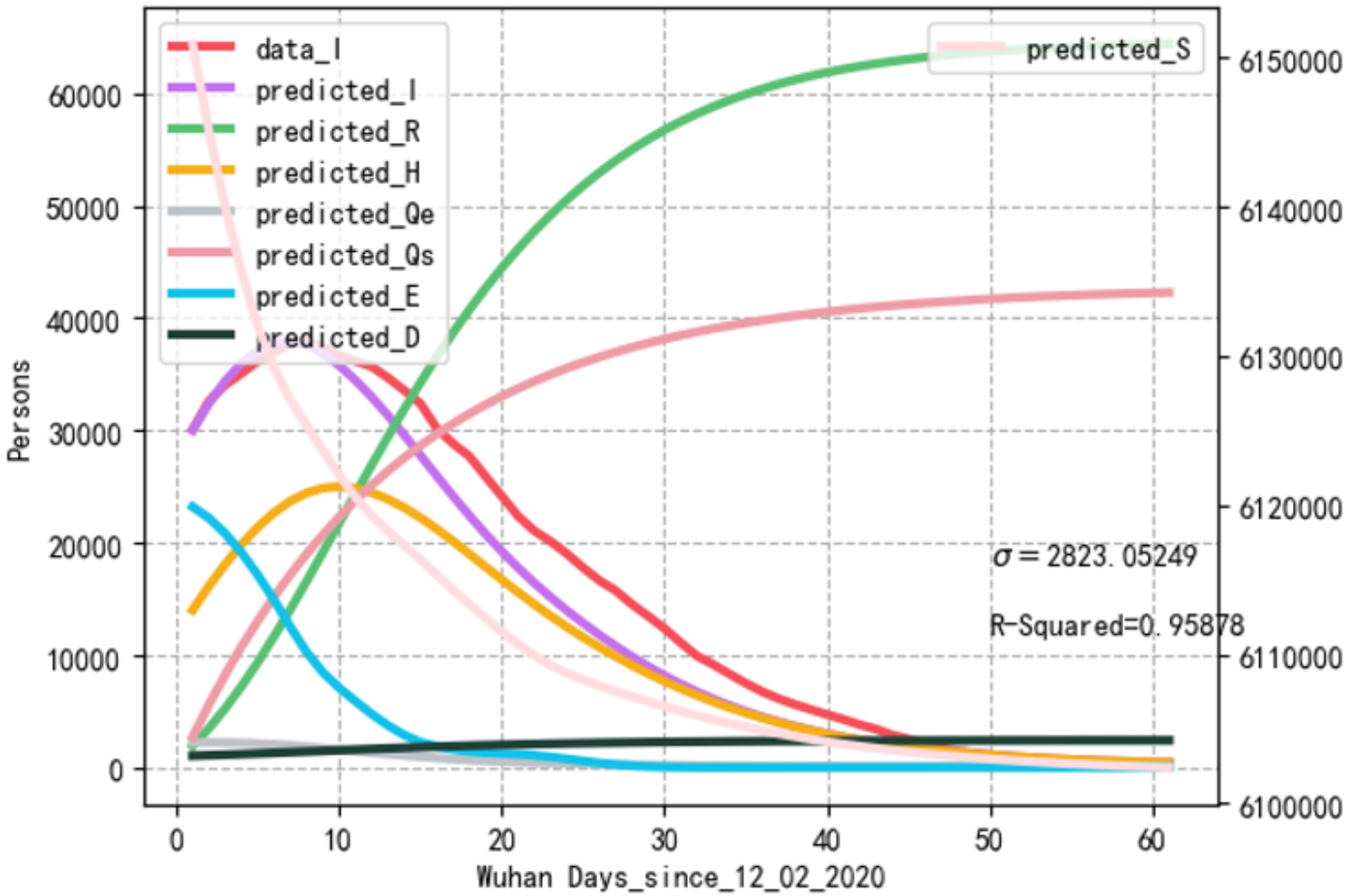

Figure 4

Simulation results in Wuhan without using AdaGrad optimizer.

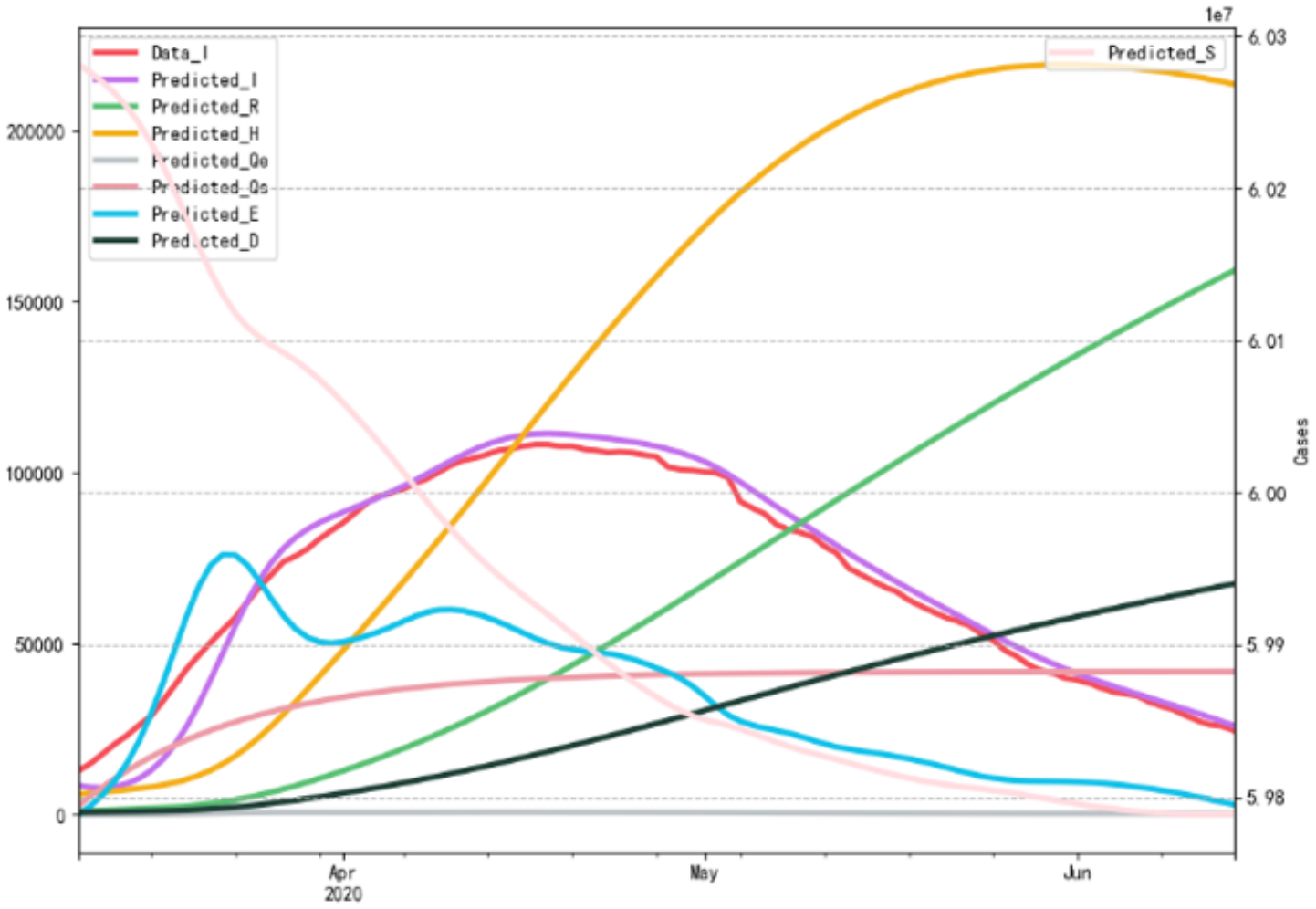

Figure 5

Simulation results for Italy

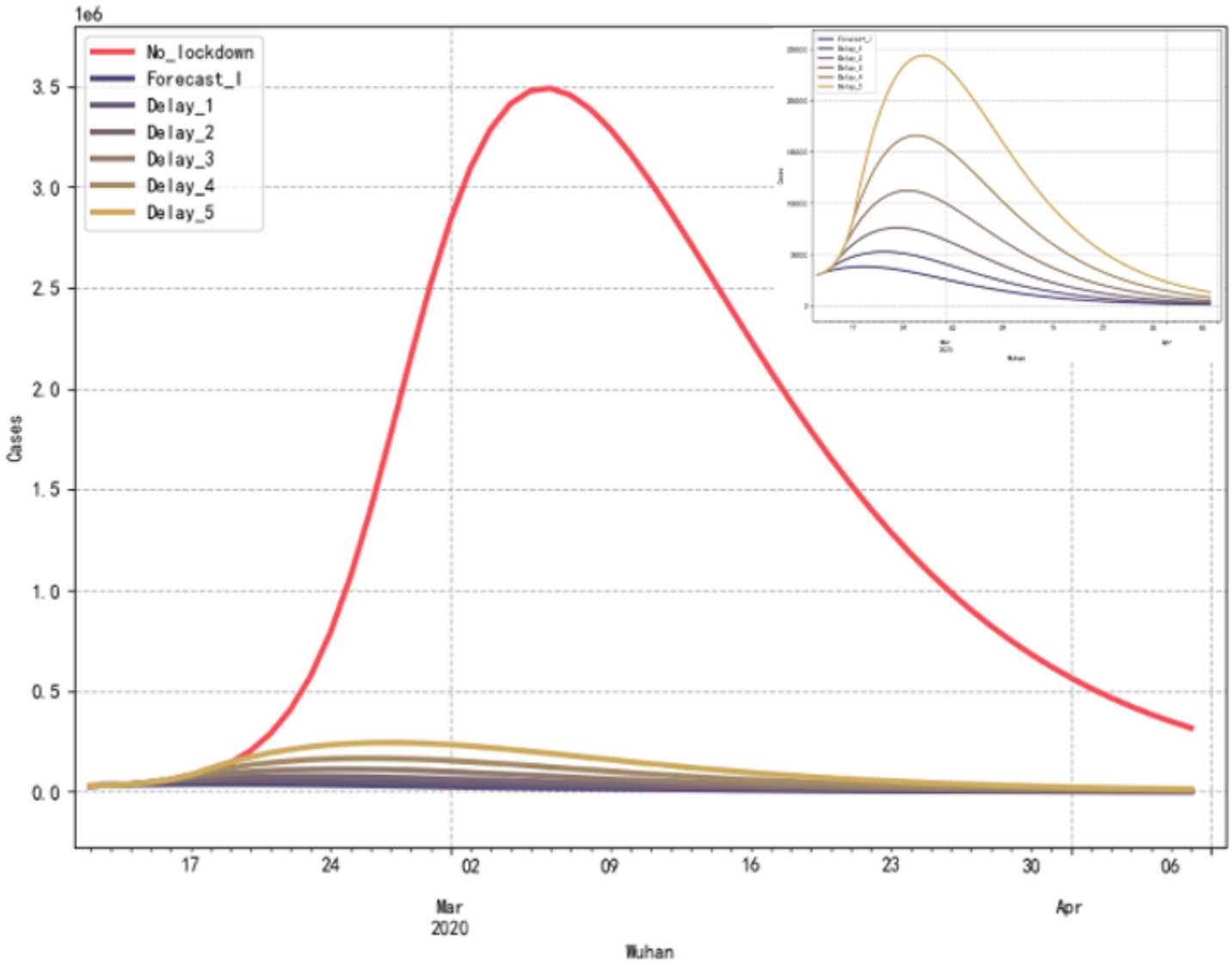

Figure 6

Simulation results of the number of infected patients when delaying the implementation of movement-restricting measures in Wuhan

Supplementary Files

This is a list of supplementary files associated with this preprint. Click to download.

- appendix.docx